CWPT Open Water Demonstration

DE-EE0008097

Budget Period 2

Task 3.2 - Belt Tradeoffs for Winch PTO

Public Report

May 2021

CalWave Power Technologies Inc.
1 Sapphire Ct, Hercules, CA 94547 +1 510-508-9897 team@calwave.energy

CONTENTS

I. INTRODUCTION

Rotary power take-offs (PTOs) promise many benefits for commercial wave energy converters (WECs), including longer power strokes/reduced end-stop concerns, deployment advantages, and controllability. However, these winch-type PTOs impose high cycle counts on the belt or rope element which may lead to a failure mode known as Cyclic Bend Over Sheave, or "CBOS". Synthetic rope, though attractive due to its high strength, low elongation, and durability, suffers from comparatively poor CBOS performance and struggles to reach millions of load cycles without failing [1, 2]. This makes synthetic ropes difficult to utilize in WECs where the number of bend cycles can easily exceed multiple millions during a single year of operation in typical wave resources.

Rope CBOS life is correlated with the life factor (LF), the product of the safety factor (SF) in a given loading condition with the D/d ratio. The safety factor is defined as the ratio of the rope's minimum breaking load (MBL) to the tension applied to the rope (T). The D/d ratio is the ratio between the sheave diameter the rope is bent around to the rope's diameter. The equation for calculating the life factor is given in (1). In general, the greater the SF and D/d ratio, the better the CBOS performance for a specific rope construction. However, the SF and D/d ratio typically have an inverse relationship, as the SF decreases with smaller rope diameters.

$$LF = SF \times \frac{D}{d} = \frac{MBL}{T} \times \frac{D}{d} \qquad (1)$$

Using belts instead of ropes for winching elements can theoretically improve CBOS performance due to having a smaller thickness that undergoes bending. The belt can be thought of as a rope that is flattened and can have the same cross-sectional area and thus breaking strength. Furthermore, for a belt, the thickness of the tension carrying element, which can be smaller than the overall belt thickness, is utilized as the belt "diameter" (d) in the D/d ratio. This allows for larger life factors to be achieved with the same cross-sectional area of tension carrying elements and sheave diameter. Unfortunately, belts have their own host of challenges. Maintaining even tension across the width of a belt subject to twist or fleet angles is a challenge, especially for WECs which can oscillate in multiple degrees of freedom under the action of waves.

CalWave Power Technologies Inc. (CalWave) assessed winch mechanism in its WEC capable of high cycles and full system loads. This report summarizes tradeoffs evaluated and lessons learned in selecting a belt for a scaled winch type PTO for open ocean deployment. Two distinct belt constructions were tested in two separate CBOS testing campaigns: High Modulus Polyethylene (HMPE) woven fiber belts and steel cable polyurethane belts.

This material is based upon work supported by the U.S. Department of Energy's Office of Energy Efficiency and Renewable Energy (EERE) under the Water Power Technologies Office Award Number DE-EE0008097.

This report was prepared as an account of work sponsored by an agency of the United States Government. Neither the United States Government nor any agency thereof, nor any of their

employees, makes any warranty, express or implied, or assumes any legal liability or responsibility for the accuracy, completeness, or usefulness of any information, apparatus, product, or process disclosed, or represents that its use would not infringe privately owned rights. Reference herein to any specific commercial product, process, or service by trade name, trademark, manufacturer, or otherwise does not necessarily constitute or imply its endorsement, recommendation, or favoring by the United States Government or any agency thereof. The views and opinions of authors expressed herein do not necessarily state or reflect those of the United States Government or any agency thereof.

II. WOVEN HMPE FIBER BELT

BELT CONSTRUCTION

CalWave collaborated with a textile manufacturer on the selection of an appropriate HMPE webbing belt. A sample of HMPE belt was supplied for testing on a CBOS testing setup at the Materials Testing Facility of the French Research Institute for Exploitation of the Sea (IFREMER). The scaled belt sample was nominally 6m long, 100 mm wide and 2.6 mm thick. The belt has a nominal breaking strength of 180 kN. End terminations were made by folding the belt end over and sewing the two sides together to create a loop, as shown in Figure 1.

Figure 1: HMPE belt construction showing end loop termination.

TESTING

Access to Ifremer's Material Testing Facility was provided through the MaRINET2 program. An HMPE belt sample as well as a new Nylon pulley sheave were supplied by CalWave to Ifremer. A single endurance testing experiment was planned for the full duration of facility access. A constant load of 90 kN was applied to the sheave, inducing a 45kN tensile load on the belt. The belt was displaced sinusoidally with an amplitude of 320 mm at a period of 14s in order to have sections of the belt fully pass on and off the sheave during each cycle. Note that this leads to two bend-unbends per cycle, whereas a belt wrapping on and off a winch drum would only have one bend-unbend per cycle. Experimental data, including applied and measured loads and piston displacements were recorded with a sampling frequency of 1 Hz. The belt was subject to a freshwater spray to imitate the thermal effects of submerged operation. An IR camera was used to compare surface temperatures between 5 points on the belt and a reference point on the sheave at intervals throughout the test. Testing was scheduled to continue constantly for 3 full

weeks although ultimately only 2 weeks of total sample excitation was achieved. The test setup is shown in Figure 2.

Figure 2: Experimental set up with sheave and belt mounted to the test machine.

RESULTS

Experiments commenced on January 15th, 2019. Consistent piston displacements and forces were achieved over multiple cycles. Aside from a single element fiber element breaking during the initial belt loading, no additional damage was noted during the first 6 days of testing and the belt was able to adequately withstand the 45kN of constant tension. However, on January 22nd, significant visible damage was first observed after 41k cycles and this damage subsequently developed along the lower belt edge. The surface temperature of the belt never exceeded 22˚ C throughout the experiment.

The test was stopped on January 25th after a total of 61k displacement cycles. The damage to the belt at this time is shown in Figure 3. Over a third of the belt displayed visible damage at this time and only 80 mm of the original 100 mm belt was still engaged with the sheave due to the remaining folding over.

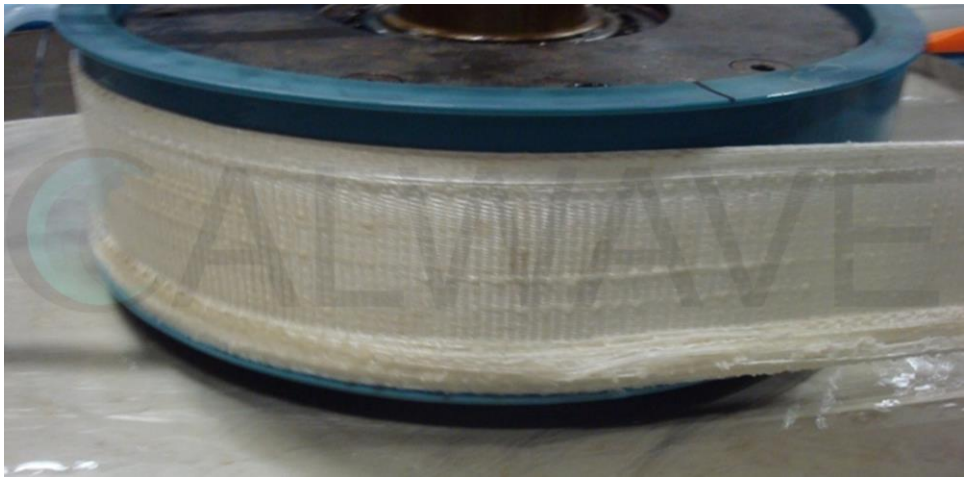

Figure 3: Damage to belt at the end of the first test. Note that the belt had also significantly slipped down the sheave.

The belt was removed for inspection. It had become very stiff in the area subjected to the cyclic bending load. Although the damage was primarily localized along the bottom edge, the upper edge also showed some signs of damage and wear.

To continue to make use of the 3-week allotted testing time and acquire more data, the sheave and belt were both flipped such that the damaged ends were on the top and reinstalled onto the machine. Testing was then restarted on January 30th following the same testing conditions. Complete belt failure occurred after 78,600 total machine cycles (157,000 bending-unbend cycles) after an additional 18k cycles since restarting the experiment caused the belt to break along its full width. The torn areas of the belt can be seen in Figure 4. The belt also exhibited some delamination upon failure suggesting a layered cross section construction as opposed to fully weaved.

Figure 4: Belt after complete failure.

ANALYSIS AND CONCLUSIONS

The belt failed prior to enduring 100k cycles and fell short of the targeted millions of cycles. However, although the intent of the experiment was to test the CBOS performance of the HMPE belt, the actual failure mechanism appeared to be caused by abrasion along the belt edges due

to the belt not fitting properly inside the sheave. A properly sized belt and sheave pair is expected to significantly increase the belt life. The delamination of the belt brings to question whether a fully woven cross section would be more robust than the layered one. It is also expected that upgrading to a branded fiber, such as DSM's Dyneema or Honewell's Spectra, could increase fiber performance. Fiber manufacturers also have developed special coatings such as DSM's XBO coating which claim improved CBOS performance. Additional testing on an improved belt and sheave that incorporates the learnings is considered before the technology can be implemented in a scaled deployment reliably.

As a secondary result, load levels and temperatures caused by this testing induced very little creep elongation of the fibers. It is possible that with a shorter oscillation period, the belt would reach higher temperatures than found in this experiment. Nevertheless, the low temperatures recorded are thought to leave sufficient margin before heating of the fibers becomes a real concern.

III. Steel Cable Polyurethane Belt

The study presented herein sought to quantify the CBOS performance of a belt consisting of steel tension members in a polyurethane matrix containing longitudinal profiles. These belt samples were tested at TMT laboratories to failure or up to two million bend-unbend cycles and under additional disturbances such as fleet angle. This section summarizes the utilized testing methodology and the resulting belt performance.

Belt Construction

The belt consists of steel tension members encased in a polyurethane matrix. A partial cross section of this belt is shown in Figure 5. The wavy longitudinal profile allows the belt to distribute off axis loads across entire face of the belt as opposed to concentrating such loads along the right or left belt edges. The belt was manufactured by vulcanizing the profiles to a base flat belt.

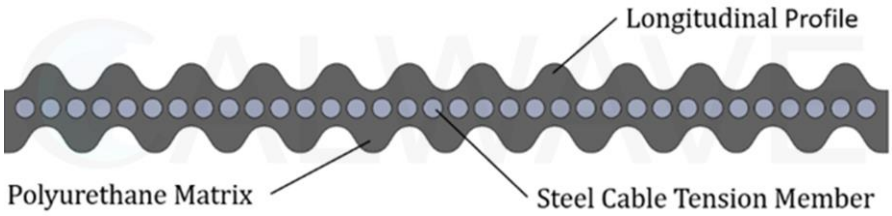

Figure 5: Cross section of steel tension member belt

Experimental Setup

A computer aided design (CAD) model of the utilized test rig is shown in Figure 6. All components are mounted to a large steel frame. Two belt samples with looped terminations are connected to each other, allowing for CBOS testing on both samples simultaneously. The belt samples each run over a respective drum that induces bending. The displacement of the belts is driven by a hydraulic motor that drives one of the drums. The other drum is coupled to a servo-controlled hydraulic cylinder that applies tension to the belt samples. The two drums are therefore referred to as the “drive drum” and “tension drum” later in this section. In this manner, the tension and displacement are controlled by separate actuators and decoupled. The connection between the drive drum and the test frame can be rotated to induce a misalignment in the system and a fleet angle on the belt, as shown in Figure 7.

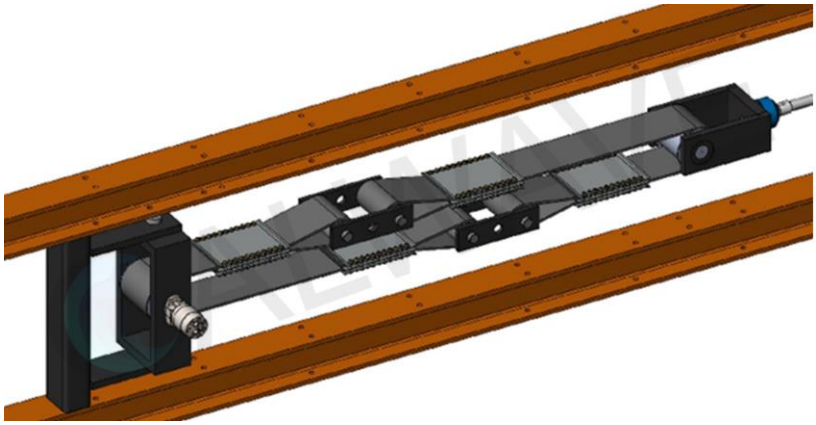

Figure 6: Model of test rig setup showing from left to right, actuating hydraulic motor, belt samples, and tensioning cylinder.

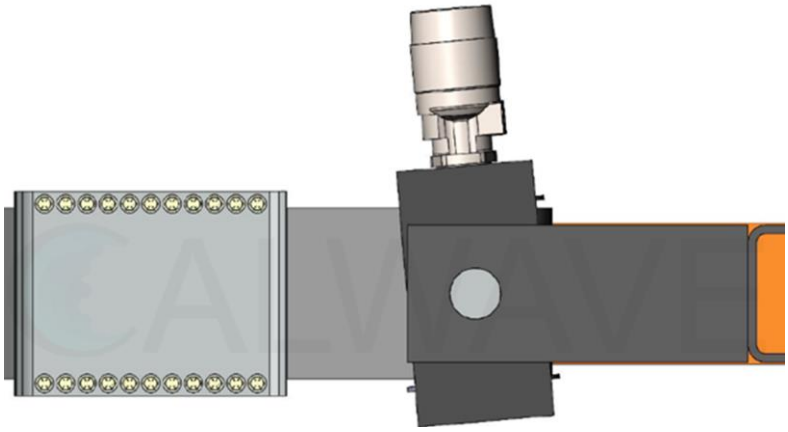

Figure 7: The drive drum can be pivoted to create a belt fleet angle. A five-degree angle is shown.

Photographs of the realized test stand with the steel cable belt samples can be found in Figures 4 - 6. A load cell is installed on the tensioning cylinder rod end to measure cylinder induced tension, shown in Figure 8. A string potentiometer measures the cylinder displacement. To help support the weight of the belt terminations, support trolleys that ride along the steel frame were added, shown in Figure 9. Infrared (IR) temperature measurement sensors were installed to measure belt surface temperature on both the drive and tension drums, as shown in Figure 10.

Figure 8: Tensioning drum clevis assembly attached to load cell and hydraulic tensioning cylinder.

Figure 9: Belt samples attached to termination support trolleys.

Figure 10: Drive drum and IR temperature sensor

For CBOS testing, the belt was oscillated with a 2 second period and 0.79m stroke. Each of these 2 second oscillations are considered a single machine cycle. The 2 second period was the shortest the test machine could run at and was selected to accelerate cycle induced failure and minimize machine usage. Note that this is more than half of an order of magnitude faster than periods typical for ocean waves. The constant 0.79m stroke was selected to concentrate the number of bending cycles undergone by the belt in a reasonably sized section.

This excitation created a 0.3m long double bend zone on each sample. The double bend zone is a section of belt that sees two bend-unbends (one on both sides of the drum) per machine

oscillation cycle. The single bend zone on either side of the double bend zone was approximately 0.49m. For some tests, a time varying force profile was requested on the tensioning cylinder. The purpose was to induce the full range of tensions that the belt would expect to see in the field, while also accounting for the probability of occurrence of each load. This profile was repeated with a period of one hour, 1800 times longer than that of the displacement. This long period simplified the force control requirements on the tensioning cylinder and ensured that tension and displacement were decoupled. Thus, all belt elements experienced the full tension profile during bending. The induced tension on the belt sample is shown in Figure 11, normalized by the manufacturer provided minimum breaking load of the belt. Note that due to the nature of the test set-up, these tensions are half the tension in the cylinder. Fleet angles were manually adjusted in a range of 0-3 degrees in between testing intervals. Dynamic variation of fleet angles was not included as part of these experiments.

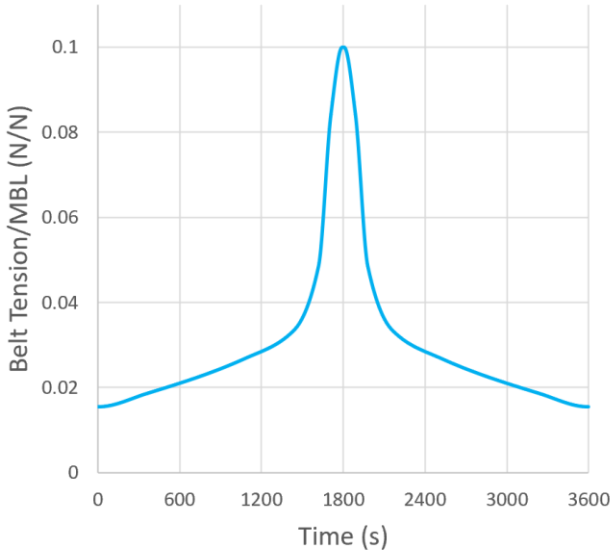

Figure 11: Belt tension profile imposed during some experiments. Tension is normalized by the minimum breaking load of the belt.

A data logger was used to continuously monitor and record the test parameters including belt tension, belt temperatures, ambient laboratory temperature, number of tension cycles, and number of machine cycles. Triggers were set to automatically pause the test should any of the measured parameters stray beyond their acceptable range. During each machine cycle, the temperature sensors captured the temperatures of both the single-bend and double-bend zones as the belts passed by their field of view. The drums and belt steel tension member diameters corresponded to a D/d ratio of approximately 91.

Testing was conducted from January 26-February 20, 2021 on a single pair of steel cable belt samples. A chronological summary of the bending machine cycles applied to the steel cable belt samples is given in Table I. Cycle blocks indicated with “Profile” tension utilize the force profile in Figure 11. Cycle blocks with a tension range had multiple constant tension tests, starting with the first number in the range and ending at the second. The remaining tests were conducted with constant tension. Tensions are normalized by the belt minimum breaking load. Thus, life factors

corresponding to the conducted tests ranged between 585 and 5850. In total, 847,612 machine cycles were applied to the belt samples, corresponding to nearly 1.7 Million bend-unbends in the double bend zone. A summary of the cumulative machine cycles applied to the belt samples, grouped by fleet angle, is provided in Table II.

RESULTS

The initial trial runs (cycle blocks 1, 2, and 3) were conducted with a drive belt fleet angle of 3 degrees. These initial runs were intended to confirm the longitudinal profiles' ability to withstand large fleet angles. These brief trial runs (only 462 total machine cycles) quickly revealed that at low belt tensions, the belt profiles climbed partially out of and then snapped back into the drum grooves with each stroke of the test rig. The lateral displacement of the belt on the drum was limited by a drum flange, so the belt ribs were unable to jump from groove to groove. Note that this type of fairlead induced oscillation test is considered the worst case as compensation by e.g. a suitable mechanical fairlead mechanism is not considered as the drum was kept rigid in place under the set fleet angle.

TABLE I
CHRONOLOGICAL BENDING TESTS

Cycle Block	Fleet Angle (°)	Normalized Tension (N/N)	Machine Cycles	Cumulative Machine Cycles
1	3.0	0.024	400	400
2	3.0	0.016	26	426
3	3.0	0.016	36	462
4	0.0	Profile	250,000	250,462
5	1.0	Profile	46,953	297,415
6	0.0	Profile	176,497	473,912
7	0.5	Profile	123,550	597,462
8	1.0	0.089	153,500	750,962
9	2.0	0.016-0.156	37	750,999
10	1.5	0.016-0.156	58	751,057
11	1.5	0.138	37,655	788,712
12	1.5	0.138-0.016	50	788,762
13	2.0	0.016-0.138	95	788,857
14	2.0	0.089	58,755	847,612

Chronological summary of excitation cycles induced on the steel cable belt samples. Tensions are normalized by the belt minimum breaking load.

To ensure that at least CBOS performance was tested, a conservative approach was selected for the remainder of the testing. The drive drum was set to a fleet angle of 0 degrees for cycle block 4, with step increases in fleet angle planned in subsequent cycle blocks. Cycle block 4 was run for a duration of 250,000 machine cycles utilizing the force profile. The belt samples appeared to be visibly undamaged at the conclusion of this cycle set.

The fleet angle was then increased to 1.0 degree for cycle block 5, and the test was resumed using the tension profile. Although initially stable, after running for 13k cycles, the ribs on the drive belt began to climb partially out of and then snap back into the drum grooves enough to trigger a machine auto-stop due to low tension. This snapping behavior did not occur in regular intervals and did not seem to correlate with sample displacement or excitation frequency. During some strokes, the sample would snap twice, while others it would not snap at all. This snapping behavior appeared to only occur when the normalized tension was below 0.078. The total duration of this cycle block was 46,953 machine cycles, after which it was determined that the snapping behavior could cause more risk for the machine and samples and that an operating condition that didn't trigger the snapping behavior would be more likely to help quantify the CBOS performance.

The drive drum was then returned to a fleet angle of 0 degrees, and cycle block 6 was conducted using the tension profile for an additional 176,497 machine cycles.

TABLE II
CUMULATIVE BENDING BY FLEET ANGLE

Fleet Angle (°)	Tension (N/N)	Total Machine Cycles
0.0	Profile	426,497
0.5	Profile	123,550
1.0	Profile and 0.089	200,453
1.5	Various	37,763
2.0	Various	58,887
3.0	0.016 and 0.024	462

Summary of total cumulative machine cycles applied to belt samples. In total 847,612 cycles were applied. Tensions are normalized by the belt minimum breaking load.

The drive drum was then set at a fleet angle of 0.5 degrees, and cycle block 7 was conducted using the tension profile for an additional 123,550 machine cycles. The belt ran smoothly with this smaller fleet angle. At this point, the cumulative number of machine cycles was 597,462. It was then decided to abandon the tension profile and continue the test with various fleet angles and with belt tensions high enough to allow smooth belt operation over the drums. On four occasions during the remaining portion of the test program, brief trial runs were made to determine the belt response to a range of tensions for specific fleet angles. The results of these trial runs were used to select the test tension for the subsequent cycle block.

For cycle block 8, the fleet angle was increased to 1.0 degree, and the normalized belt tension was set to 0.089. The duration of this cycle block was 153,500 machine cycles. The temperature of the drive belt sample remained approximately 3 degrees C above the temperature of the tension belt sample. By the end of cycle block 8, wear from a total of 750,962 cycles had accumulated on the belt samples. The photographs in Figures 8 and 9 show the drive belt sample wear debris accumulated by the end of cycle block 8. The accumulated belt debris was mainly the result of belt rib wear produced as one side of each rib rubbed against the mating side of its drum groove. The lateral thrust of the belt ribs against the drum grooves was due to the belt fleet angle. Note that this debris was not artificially disturbed throughout the series of tests. The tension belt sample appeared undamaged at the end of cycle block 8.

The fleet angle was then increased to 2.0 degrees. A brief trial run (cycle block 9) revealed a loud abrasive sounding noise made by the belt sample over the full range of acceptable belt tensions. This was deemed unacceptable behavior and the fleet angle was then decreased to 1.5 degrees. Another brief trial run (cycle block 10) revealed that normalized tensions above 0.058 prevented jumping behavior of the belt, and tensions above 0.138 reduced the abrasive noise.

Cycle block 11 was then conducted with the 1.5-degree fleet angle and a normalized belt tension of 0.138 for 37,655 machine cycles. After a few hours, the abrasive sound completely disappeared and the belt ran quietly. The temperature of the drive belt increased from approximately 10 degrees C to approximate 15 degrees C above the temperature of the tension belt, likely due to

a changing belt wear pattern on the drum. The photographs in Appendix D show the belt wear debris accumulated by the end of this cycle block at a total of 788,250 machine cycles.

Figure 12: Drive belt wear in double bend zone after 750,962 cycles. Greatest wear on the near edge of the belt.

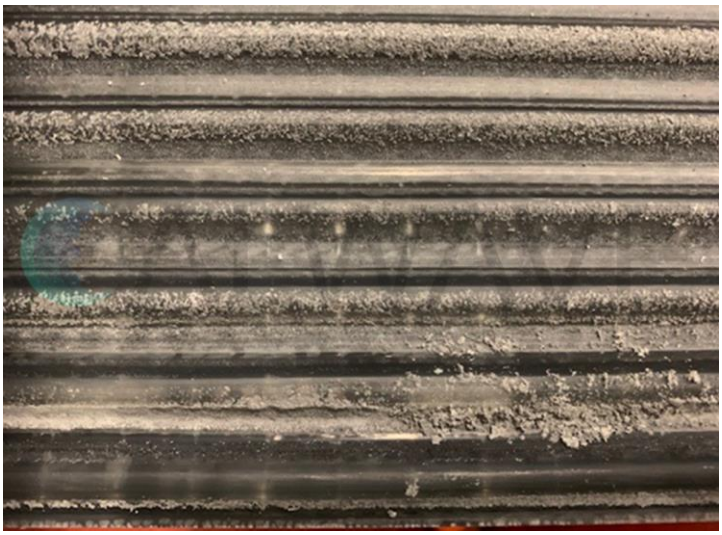

Figure 13: Close up of Figure 12 showing wear. Accumulated powder residue thought to be worn polyurethane debris.

A brief trial run (cycle block 12) was then conducted with the same 1.5-degree fleet angle and the full range of belt tensions. This time, the belt operated smoothly without jumping or with excessive noise at all tensions. The fleet angle was then increased to 2.0 degrees, and another brief trial run (cycle block 13) revealed that the belt continued to run smoothly at all tensions, likely due to the wear previously experienced by the belt ribs.

The test was then continued with the 2.0-degree fleet angle at a normalized belt tension of 0.089 (cycle block 14). At about one-quarter of the way through this cycle block, the maximum temperature of the drive belt was approximately 30 degrees C above that of the tension belt. At

the cycle block progressed, the temperature difference diminished to approximately 25 degrees, likely due a changing belt wear pattern on the drum. The test was stopped after a cumulative total 847,612 machine cycles. This final cycle block produced enough additional belt wear to expose two steel cables on the belt face at the high-tension edge, shown in Figure 14. Another steel cable was exposed along the low-tension edge of the belt due to contact with the drum flange. Resulting polyurethane wear residue can be seen on the belt sample in Figure 15 and on the drive drum in Figure 16. The test was deemed complete at this point because of the belt damage. The companion belt sample on the tension drum remained undamaged at the end of the test program.

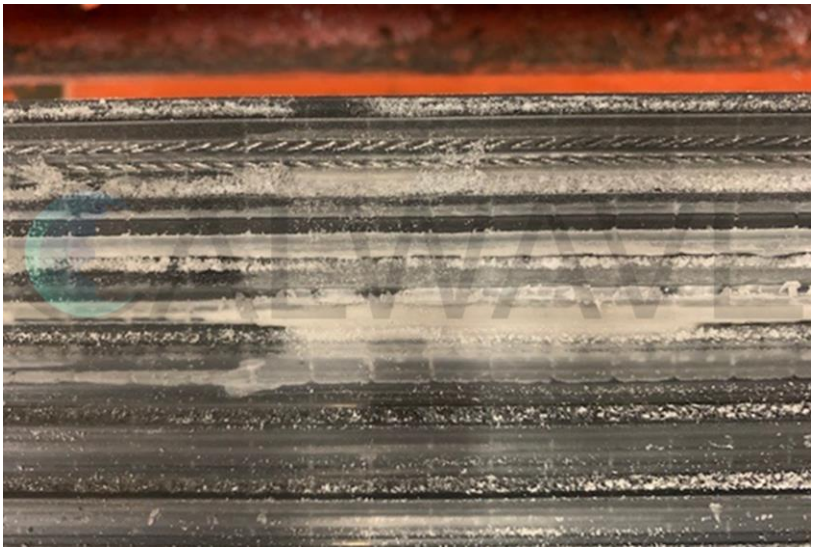

Figure 14: Exposed steel cables at 847,612 machine cycles.

Figure 15: Belt wear residue at 847,612 machine cycles.

Figure 16: Belt wear debris in drum grooves at 847,612 machine cycles.

Since the samples did not fail due to CBOS, it was not clear how much CBOS related damage was accumulated by the steel tension members throughout this testing campaign. X-ray imaging was utilized to try to look for breaks in the cable wires in collaboration with Sandia National Laboratories' Non-Destructive Testing Laboratory. An example of the imaging results is shown in Figure 17. Review of the imaging data is still ongoing at the time of this report, but preliminary results did not find any evidence of breakages in the cable wires.

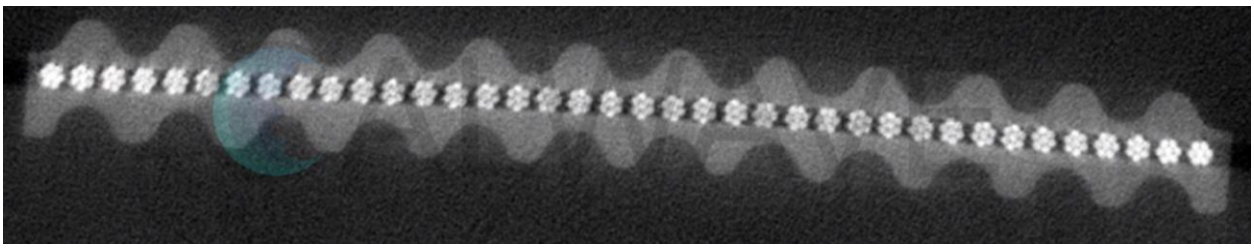

Figure 17:Example x-ray image of profiled belt after testing.

ANALYSIS AND CONCLUSIONS

From a strict CBOS perspective, the samples performed very well. The belt sample on the tension drum endured all 847,612 cycles without failing or showing visible signs of wear. This experiment showed that in addition to CBOS, wear of the belt polyurethane caused by fleet angle induced off-axis loads could ultimately determine component life. In an actual WEC deployment, exposed steel tension members would be subject to corrosion and necessitate belt replacement. Even with the longitudinal profiles, the belt had difficulty maintaining engagement with the drum at fleet angles of 1 degree and larger.

Nevertheless, it should again be highlighted that an additional degree of freedom via a suitable mechanical fairlead assembly can significantly reduce the abrasion effect compared to full oscillation with a set, enforced fleet angle as it was the case for the presented set of experiments.

Another interesting lesson learned from the study was that although higher belt tensions should theoretically be worse due to CBOS, tensions that are too low can lead to belt instability when fleet angles are present. Acceptable belt performance for the intended application will likely necessitate strict limitations on belt fleet angles.

There were some limitations to this study that could be investigated further in future work. While these tests were run dry, in actual operation, the belts are intended to be used in a wet environment. Operating in a wet environment could reduce the abrasion experienced by the belt as well as reduce some of the noise caused by the belt rubbing against the drum.

Because the samples did not fail due to CBOS, x-ray imaging was utilized to gain insight into how much CBOS related damage was accumulated by the steel tension members throughout this testing campaign. Alternative non-destructive testing (NDT) methods that could have been used to investigate the cable health include electrical resistance testing and magnetic flux leakage. Such methods may be considered in the future for monitoring belt health.

Belt sample lengths and displacement amplitudes were purposefully kept short to focus on CBOS. With an improved understanding of fleet angle effects, it is suggested that future tests include longer belt samples to reduce end effects and allow the inclusion of longer belt stroke amplitudes. Longer samples would likely improve the load sharing among the steel cables across the width of the belt for non-zero fleet angles.

Some improvement in belt performance might also be possible with changes in the belt rib and drum groove profiles. Perhaps a more trapezoidal shape for the belt ribs, such as used for V-belts, might offer greater wear area and reduced contact pressure on matching drum grooves. It is notable that the belt behavior and stability under the same test conditions changed over time, such as between cycle blocks 9 and 14. One potential explanation is that the polyurethane wear created a more optimal geometry to handle the fleet angles in question.

Finally, for simplicity, the test rig was designed to be run with fixed fleet angles. In practice, the fleet angle in a WEC system will vary and change with WEC excitation. It is of interest how dynamically varying fleet angles would improve or even hurt belt life compared to the tested conditions in this study.

IV. LESSONS LEARNED

Comparing the results from the two sets of experiments, the steel cable polyurethane belt does appear to outperform the HMPE woven fiber belt, withstanding more than 10 times the number of bending cycles without any obvious sign of CBOS fatigue. It should be noted that the two tests do have differences that make it difficult to make a fair 1:1 comparison. The HMPE fiber belt underwent constant high tension, while the steel cable belt experienced a load profile that was more realistically distributed. And due to the dimensional inconsistency with the sheave, the HMPE fiber belt was likely subject to more abrasion. However, it is difficult to see these issues fully accounting for the 10 times difference in achieved bending cycles, especially when the steel cable polyurethane belt was additionally subject to fleet angles.

Although both tests sought to quantify CBOS performance, both samples ultimately failed due to abrasion. This highlights the importance of carefully considering and implementing protective

measures against abrasion in high cycle applications. Abrasion resistant coatings or formulations of HMPE or polyurethane are potential options.

The experiments performed with the steel cable polyurethane belts proved the importance of considering and understanding all system aspects that affect belt loads, including those due to fleet angles and twist. Even with the longitudinal profiles, the belt was not able to run with a fleet angle of 3° or more without transverse travel on the drum under the fixed fleet angle conditions. Although not tested in these experiments, belt twist needs to occur over a sufficient length to keep the tension distribution across the steel tension members from being heavily skewed towards the outer members. For a winch type PTO application in Wave Energy, where one end of the belt termination can be subject to motions in multiple degrees of freedom, this underscores the need to have a method to guide the belt and prevent excessive twist and/or fleet angles via a suitable fairlead assembly.

V. REFERENCES

[1] P. Davies, N. Lacotte, G. Kibsgard, R. Craig, D. Cannell, et al.. “Durability of fibre ropes for deep sea handling operations,” in 32nd International Conference on Ocean, Offshore and Arctic Engineering, OMAE2013, Jun 2013, Nantes, France. ff10.1115/OMAE2013-11332ff.

[2] Peter Davies, Nicolas Lacotte, Maël Arhant, Damien Durville, Abderrahim Belkhabbaz, et al.. “Improved bend over sheave durability of HMPE ropes for deep sea handling,” in 37th International Conference on Ocean, Offshore and Arctic Engineering, Jun 2018, Madrid, Spain. ff10.1115/OMAE2018-77530ff.